Finite-temperature liquid-quasicrystal transition in a lattice model

Z. Rotman and E. Eisenberg
Raymond and Beverly Sackler School of Physics and Astronomy, Tel Aviv University, Tel Aviv IL-69978, Israel
(Received 5 September 2010; published 24 January 2011)

We consider a tiling model of the two-dimensional square lattice, where each site is tiled with one of the 16 Wang tiles. The ground states of this model are all quasiperiodic. The systems undergoes a disorder to quasiperiodicity phase transition at finite temperature. Introducing a proper order parameter, we study the system at criticality and extract the critical exponents characterizing the transition. The exponents obtained are consistent with hyperscaling.

DOI: 10.1103/PhysRevE.83.011123 PACS number(s): 64.60.De, 61.44.Br, 64.60.Cn

It has been known for a while that the two- or three-dimensional space may be tiled by ordered but aperiodic tilings, in addition to periodic lattice structures [1]. This aperiodic order is realized in nature by certain alloys, called quasicrystals [2,3], which are believed to exhibit in thermal equilibrium aperiodic crystalline order [4,5], i.e., long-range positional order lacking any periodicity. Aperiodic tiling models exhibiting long-range positional order are extensively used to analyze quasicrystals at zero or finite temperature [6–8]. However, understanding of the transition region between the disordered (fluid) phase and the quaicrystal phase is still incomplete.

Here we consider a model of interacting tiles on a square, two-dimensional, lattice. The model has been previously studied in Refs. [9,10]. Each site of the square lattice is tiled with a tile, characterized by four labels attached to its edges. The labels take one of possible six labels (or colors). The interaction is with nearest neighbor tiles, and the bond energy is zero if the labels of both neighboring edges match, or one otherwise. It was found by Ammann [1] that if one limits the allowed tiles to a group of 16 tiles (out of all the possible 6^4 tiles), then all zero energy states of the model (also known as perfect tilings) are nonperiodic. The 16 Ammann tiles are presented in Fig 1. The perfect tilings are then the ground states of this system. Their nonperiodicity can be shown using a mapping of the six tile labels into one of two symbols: S for labels {1,2} and L for labels {3,4,5,6}. Since all Ammann tiles have labels belonging to the same set (S or L) on both horizontal (vertical) edges, the mapping thus classifies the 16 tiles into four types according to their set along each axis: {1} S-S, {2,3,4,5} S-L, {6,7,8,9} L-S, and {10,11,12,13,14,15,16} L-L. Identifying the symbols S and L with the short (S) and long (L) Fibonacci tiles, it follows from the properties of the Ammann tiles that any perfect tiling is mapped into a two-dimensional square Fibonacci tiling [11], thus aperiodic.

The finite temperature behavior of this tiling model was studied numerically in Ref. [9]. The model has multiple ground states (uncountable infinite number for the infinite plane), all are aperiodic, and thus its dynamics upon fast cooling was suggested to be a model for glassiness. The lattices studied in Ref. [9] were in the range $8 \leqslant N \leqslant 32$ (N being the lattice linear size) with free boundary conditions. Numerical results supported the existence of a phase transition, measured by a growing peak in the specific heat, and the transition was concluded to be of second order. Recently [10], it was shown that the phase transition observed in Ref. [9] is a disorder (fluid) to quasicrystal transition. Phase-transition analysis in Ref. [10] followed an analytical approach supported by numerical simulations. The transition was studied using the overlap of a configuration with a ground state γ. The fraction of tiles in a configuration c matching a ground state γ is denoted $\phi(c,\gamma)$. The overlap, normalized by its averaged over all ground states $\psi(c) = \int \phi(c,\gamma)\, d\lambda(\gamma)$, is then thermally averaged to yield Q_β:

$$Q_\beta(\gamma) = \frac{1}{Z} \int \frac{\phi(c,\gamma) e^{-\beta H(c)}}{\psi(c)}, \tag{1}$$

where the integration is over configurations c (ensemble averaging), $H(c)$ is the energy of the configuration, and Z is the partition function $Z = \int \exp[-\beta H(c)]$. The high-temperature limit of Q_β is, by normalization, 1.

To account for the infinite number of ground states, Koch and Radin defined the quantity q_{RK}:

$$q_{\mathrm{RK}}(\beta) = -\int Q_\beta(\gamma) \ln[Q_\beta(\gamma)]\, d\lambda(\gamma), \tag{2}$$

and then $q_{\mathrm{RK}}(\beta \ll \beta_c) = 0$. Analytical calculation showed that q_{RK} vanishes identically for sufficiently high finite temperatures. Numerical simulations were then used to show q_{RK} does not vanish for low temperatures, thus proving the existence of a transition. Simulations presented in Ref. [10] employed fixed boundary conditions corresponding to a specific ground state σ. Then, the overlap of the configuration with the chosen ground state σ was used to approximate q_{RK} at low temperatures, where it is expected to contribute dominantly. Looking at system sizes $32 \leqslant N \leqslant 256$, they concluded that the transition is of third or higher order. In addition, it was suggested that the transition has no renormalization fixed point.

Square Fibonacci quasicrystals are known to exhibit distinct delta-function peaks in the Fourier transform, in a similar fashion to the peaks observed in a crystalline solid [11]. We therefore suggest using the weights of these distinct peaks to define an order parameter for the disorder-to-quasicrystal transition, one that is simpler and easier to access numerically then q_{RK}. Many frequencies show a peak, and all are irrational and related to the "golden mean" $\tau = (1+\sqrt{5})/2$. The wavevector chosen for this study is $\vec{k}_0 = ((\tau-1)/\tau,(\tau-1)/\tau)$, but results are similar for all

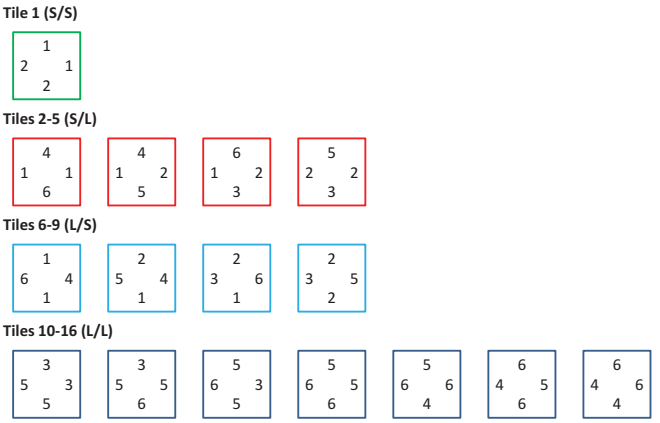

FIG. 1. (Color online) The 16 Ammann tiles. The four rows correspond to the four types of tiles (see text).

related frequencies. The (complex) order parameter is then the amplitude of the peak at $\vec{k}_0$:

$$q = \int e^{i\vec{k}_0\cdot\vec{r}}\delta_{\sigma_{\vec{r}},1}\,d\vec{r}. \tag{3}$$

Tile 1 is chosen for simplicity, as it is the only tile that is the only one of its type, i.e., it is the only tile with both edges being *S* edges. Similar results are obtained using any other type, e.g., tiles 2–5, 6–9, or 10–16.

In this paper we present numerical simulations for $10 \leqslant N \leqslant 400$ and free boundary conditions. We start by presenting the details of our numerical calculation. All simulations start from a ground state and then are thermalized at the desired temperature. Thermalization during cooling was found to be significantly less efficient. We first conducted a series of relatively short [10^6 Monte Carlo Steps (MCS)] runs in order to determine relaxation and autocorrelation times. We found that even for the largest system studied ($L = 400$), the relaxation time did not exceed 10^6 MCS. Accordingly, we discarded from all runs the first 1.6×10^6 MCS. Autocorrelation times of the order parameter were found to be much longer then those for energy and increased as much as 5×10^4 MCS

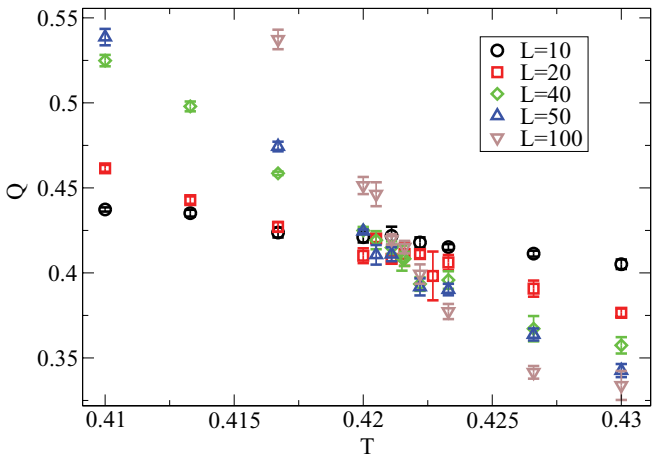

FIG. 2. (Color online) Binder cumulant of the tiling model. The collapse of crossings for various lattice sizes signals the location of the critical point.

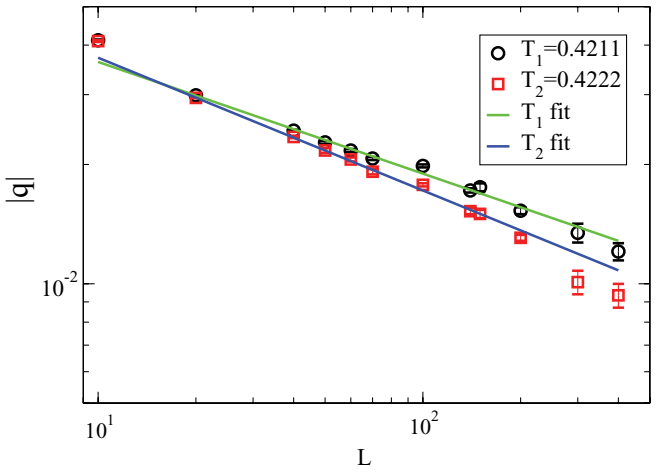

FIG. 3. (Color online) Order parameter measurements performed at T_1 and T_2. Power-law behavior is fitted, $L = 10$ is excluded from the analysis. Fitted exponents are 0.28 and 0.33.

for the largest system. The statistical measurement error was estimated based on the splitting of the measured time series into 10 parts. Each part was at least 100-fold longer than the measured autocorrelation, and thus we considered these parts as independent samplings of the variable's equilibrium distribution. To account for multiple ground states and to ensure good coverage of phase space we repeated the analysis for at least three different runs starting from different ground states for each temperature and lattice size. The measured variables were then averaged over all runs, and the error estimated based on the scatter among measurements along the runs as well as between different runs. Finite-size-scaling analysis was used to calculate the critical temperature and critical exponents of the phase transition. As expected, the error bars depend strongly on lattice size L, and thus we used weighted least square fits in order to fit the data to the finite-size-scaling forms and estimate the critical exponents. Error bars in fitted exponents are based on errors supplied by the fitting procedure, as well as robustness tests against removal of extremal points.

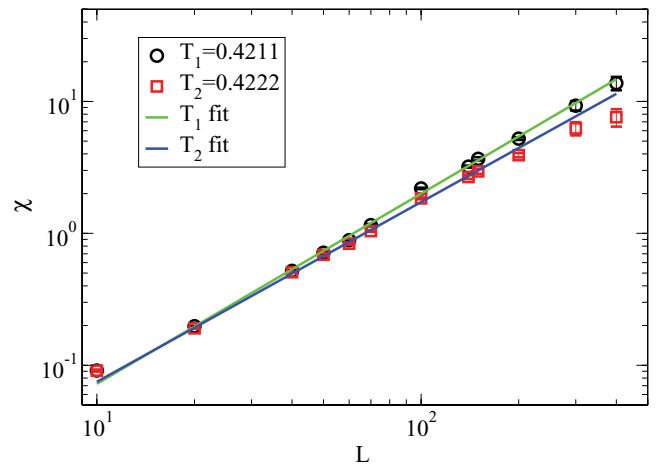

FIG. 4. (Color online) Susceptibility χ fitted to a power-law behavior at T_1 and T_2. Fitted exponents are 1.44 and 1.36.

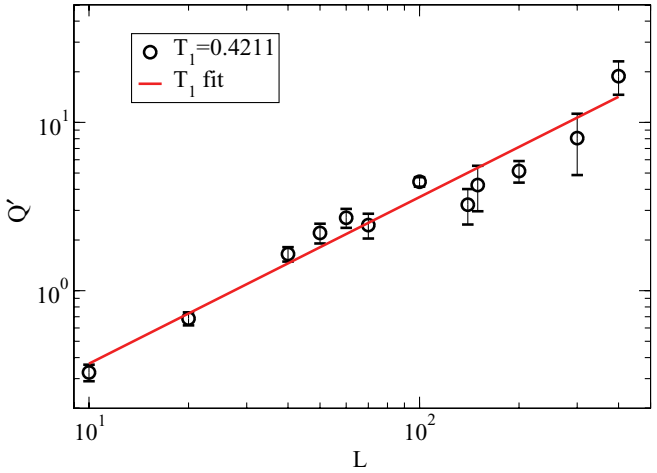

FIG. 5. (Color online) Measurements of Q' for $T_1 = 0.4211$. Fitted exponent is 0.99.

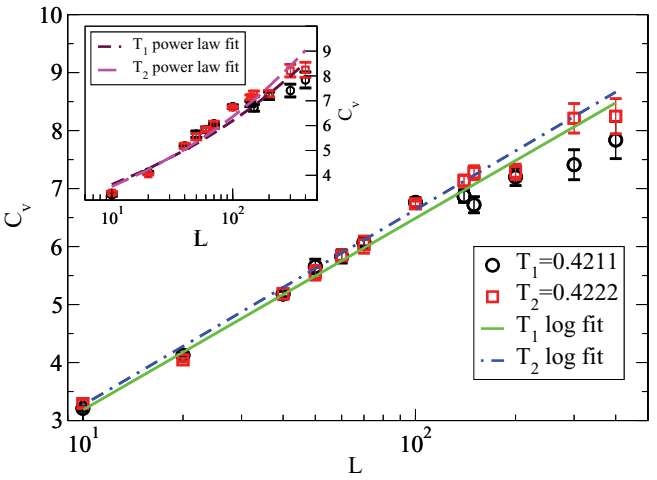

FIG. 6. (Color online) Specific heat measurements at T_1 and T_2. Data are well fitted by a logarithmic function. For comparison, best power-law fits are presented in the inset, yielding exponents 0.23 and 0.25.

In order to determine the critical temperature, we analyzed the Binder cumulant [12]:

$$Q = 1 - \frac{\langle |q|^4 \rangle}{\langle 3|q|^2 \rangle}, \tag{4}$$

where $\langle \cdots \rangle$ denotes ensemble average. Crossings of Q for system sizes $10 \leqslant N \leqslant 100$, presented in Fig. 2, show no significant finite size effects within our accuracy. The relatively large error estimates due to the long relaxation processes allow for a moderate accuracy in fixing the critical temperature, which is estimated to be $T_c = 0.4216(5)$ (here and elsewhere in this paper the number in parentheses is the uncertainty in the last digit). The critical temperature found is in agreement with previous estimates: $T_c = 0.42(1)$ [9] and $\beta_c = 1/T_c \approx 2.4$ [10]. We then studied larger lattices at two temperatures near criticality, $T_1 = 0.4211$ and $T_2 = 0.4222$. Finite size scaling of thermodynamic quantities at T_c provides estimates for the critical exponents. In this paper we verify that the critical exponents obtained for T_1 and T_2 are similar, in order to ensure that our inaccuracy in T_c does not take us out of the critical regime for the lattice sizes studied. The order parameter $|q|$ is expected to scale as $\langle |q| \rangle(L) \sim L^{-\beta/\nu}$. Figure 3 presents numerical results from measurements at T_1 and T_2 and fits to the power-law form. Based on the two fits we estimate $\beta/\nu = 0.30(3)$. Similarly, the susceptibility defined by

$$\chi = \frac{N^2(\langle |q|^2 \rangle - \langle |q| \rangle^2)}{T} \tag{5}$$

was also measured at T_1 and T_2 and fitted to the scaling form $\chi \sim L^{\gamma/\nu}$ (Fig. 4). Estimation of γ/ν from the two fits leads to $\gamma/\nu = 1.40(5)$. Note that these two independent measurements satisfy the hyperscaling relation $2\beta/\nu + \gamma/\nu = d$.

In order to estimate the critical exponent ν, we studied the derivative of the binder cumulant (Q) with respect to the inverse temperature β. Based on finite-size-scaling arguments,

$$Q' = \left. \frac{\partial Q}{\partial \beta} \right|_{T=T_c} \tag{6}$$

is expected to diverge like $L^{1/\nu}$. It is easy to see that this derivative is obtained from the energy and order-parameter moments in the following form:

$$Q' = \frac{2\langle q^4 \rangle \langle q^2 E \rangle / \langle q^2 \rangle - \langle q^4 E \rangle - \langle q^4 \rangle \langle E \rangle}{3\langle q^2 \rangle^2}. \tag{7}$$

Measurements presented in Fig. 5 indeed show a power-law behavior of $Q'(N)$, and the exponent estimated is $1/\nu = 1.05(15)$. This value for ν is consistent with measurements of the specific heat:

$$C_v = \frac{\langle E^2 \rangle - \langle E \rangle^2}{N^2 T^2}, \tag{8}$$

which are best fitted by a logarithmic growth (Fig. 6), i.e., $\alpha = 2 - d\nu = 0$, or $\nu = 1$. The results are consistent with the analysis performed in Ref. [9], leading to $\nu = 1.6(5)$.

In conclusion, we show that the use of the Bragg peak allows for an analysis of the disorder to quasicrystal transition in a two-dimensional lattice model based on Ammann tiles. The transition occurs at a finite temperature and is of a second order. Critical exponents were measured and shown to satisfy hyperscaling relations. This model is therefore suitable for study of the critical emergence of quasiperiodic order.

We are grateful to Ron Lifshitz for important discussions and insightful comments and to Hans Koch for providing useful information regarding the numerical simulations as well as a critical reading of the manuscript.

[1] B. Grünbaum and G. Shephard, *Tilings and Patterns* (Freeman, New York, 1987).
[2] D. Shechtman, I. Blech, D. Gratias, and J. W. Cahn, Phys. Rev. Lett. **53**, 1951 (1984).
[3] R. Lifshitz, Found. Phys. **33**, 1703 (2003).
[4] R. Lifshitz, Z. Kristallogr. **222**, 313 (2007).
[5] C. Janot, *Quasicrystals: A Primer* (Oxford University Press, Oxford, 1992).
[6] *Physical Properties of Quasicrystals*, edited by Z. M. Stadnik (Springer, Berlin, 1999).
[7] J. B. Suck, M. Schreiber, and P. Hussler, *Quasicrystals: An Introduction to Structure, Physical Properties and Applications* (Springer, Berlin, 2002).
[8] *Quasicrystals: Structure and Physical Properties*, edited by H.-R. Trebin (Wiley-VCH, Weinheim, 2003).
[9] L. Leuzzi and G. Parisi, J. Phys. A **33**, 4215 (2000).
[10] H. Koch and C. Radin, J. Stat. Phys. **138**, 465 (2010).
[11] R. Lifshitz, J. Alloys Compd. **342**, 186 (2002).
[12] K. Binder, Z. Physik B **43**, 119 (1981); Phys. Rev. Lett. **47**, 693 (1981).